Volume 14
Number 12
28 March 2022
Pages 4351-4772

Nanoscale

rsc.li/nanoscale

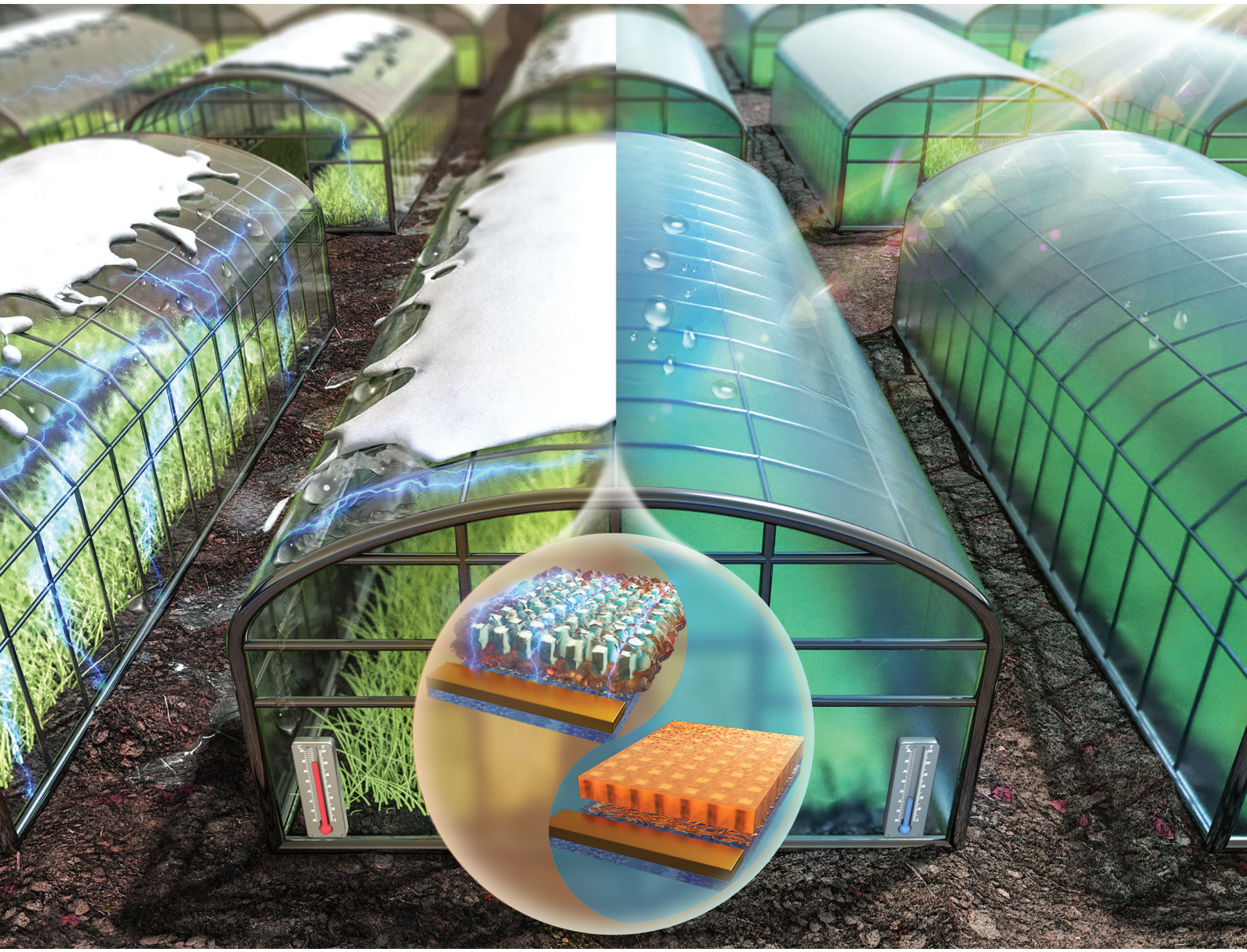

ISSN 2040-3372

ROYAL SOCIETY OF CHEMISTRY

PAPER

Chao Chen, Yachao Zhang *et al.*

A dual-mode laser-textured ice-phobic slippery surface: low-voltage-powered switching transmissivity and wettability for thermal management

NCNST

Nanoscale

PAPER

View Article Online
View Journal | View Issue

Check for updates

Cite this: *Nanoscale*, 2022, **14**, 4474

A dual-mode laser-textured ice-phobic slippery surface: low-voltage-powered switching transmissivity and wettability for thermal management†

Chao Chen, *[a] Yan Chen,[b] Hao Yao,[a] Qingrui Song,[c] Chong Jia[a] and Yachao Zhang*[d]

Smart windows that dynamically fine-tune the solar energy gain are promising candidates for alleviating the global energy crisis. However, current smart surfaces easily deteriorate when rain or frozen ice dwells on the surface structure, heavily hindering their applications. Here, we report an electric-powered dual-mode slippery lubricant-impregnated porous surface (DM-SLIPS) developed by integrating paraffin wax and laser-ablated polytetrafluoroethylene (LA-PTFE) along with a silver nanowire thin-film heater. Owing to its fast electrical response, DM-SLIPS can be switched to repel surface-dwelling liquids within 20 s by applying an ultra-low voltage of 6 V. Simultaneously, light irradiated on DM-SLIPS can be finely-tuned between a "lock mode" and "release mode" in response to the solidification/liquidation of paraffin. Owing to homogeneous Joule heating, the DM-SLIPS surface can remove surface-frozen ice within 4 min *in situ*. As a proof-of-concept, the temperature of an indoor object shielded with electric-actuated DM-SLIPS could be reversibly switched between 34 °C and 29 °C, realizing controllable solar energy input. In comparison with previously reported surfaces, the present water-repellent, ice-phobic and transparency-switchable DM-SLIPS can be more useful for thermal management in extreme climates.

Received 3rd December 2021,
Accepted 2nd February 2022

DOI: 10.1039/d1nr07940a

rsc.li/nanoscale

Published on 04 February 2022. Downloaded on 8/10/2024 8:31:31 AM.

1. Introduction

Designing improved energy-saving smart materials is an active research topic in material science because of the increasing concerns related to energy consumption and sustainable development. It is known that residential buildings are accountable for almost 30% to 40% of primary energy consumption in the world.[1] Switchable smart windows can modulate the transmittance of solar radiation in response to external stimuli, making them very promising tools for improving the energy utilization efficiency of buildings.[2] Thus, a series of temperature- or electricity-triggered smart surfaces based on various principles, including electrochromism,[3–8] thermochromism,[9–12] and liquid crystal alignment,[13–17] have been developed for finely-tuning solar transmittance. Unfortunately, these smart windows are easily impeded by liquid-based contaminants, which heavily deteriorate the surface dynamic glazing performance. In this regard, new smart surfaces boosted with switchable wettability and transparency to address the above-mentioned obstacles are currently an urgent need.

With this in mind, Aizenberg and co-workers showcased the first concept of an adaptive slippery liquid-infused porous polytetrafluoroethylene (PTFE) surface (SLIPS) with tunable optical transmittance and wettability in response to a graded mechanical stimulus.[18] By alternately applying and removing mechanical stretch, the surface feature could be finely tuned between a sticky undulating state (Wenzel's mode) and a slippery flat one (Cassie's mode), thereby pinning/slipping surface liquids accompanied by dynamic glazing. By following this classical strategy, they prepared a temperature-responsive SLIPS by doping paraffin wax into a polydimethylsiloxane matrix, which could switch the optical and wetting properties by melting/solidifying the paraffin wax.[19] As such, Manabe *et al.* developed a thermo-activated SLIPS using layer-by-layer self-assembly, and its light transparency and liquid wettability on the surface could be switched at room temperature by opti-

[a]*Department of Materials Physics and New Energy Device, School of Materials Science and Engineering, Hefei University of Technology, Hefei 230009, China. E-mail: chaoc11@ustc.edu.cn*
[b]*Department of Polymer Materials and Engineering, School of Materials and Chemical Engineering, Anhui Jianzhu University, 230601, China*
[c]*Institute of Tribology, Hefei University of Technology, Hefei 230009, China*
[d]*CAS Key Laboratory of Mechanical Behavior and Design of Materials, Department of Precision Machinery and Precision Instrumentation, University of Science and Technology of China, Hefei 230026, China. E-mail: zyachao@ustc.edu.cn*
†Electronic supplementary information (ESI) available. See DOI: 10.1039/d1nr07940a

This journal is © The Royal Society of Chemistry 2022

Published on 04 February 2022. Downloaded on 8/10/2024 8:31:31 AM.

mizing the ratio of solid paraffin and liquid paraffin oil hybrid.[20] Though ceaseless efforts have been dedicated to advancing the experimental and theoretical understanding of SLIPS-based smart surfaces,[31] several problems arise subsequently. (1) The reduplicative mechanical stretch and the volatile lubricant (perfluoropolyether) lead to short longevity in mechanically triggered SLIPS, impeding its long-term usage as an optical and wetting manipulator.[18] (2) The switching strategy is limited to an *ex situ* hot plate/oven with pronounced voltage (*e.g.*, 220 V), which is not portable and energy-consuming.[19,20] (3) In extremely cold winter, the surface-frozen ice, with strong light-scattering and large IR emittance, is not favorable for solar energy gain and storage.[18–20] In this consideration, integrating the features of ice-phobicity, liquid repellency and dynamic glazing into one single SLIPS for *in situ* thermal management under extreme climates (*e.g.*, snowy winter, dim rainy days) is highly desirable yet challenging to date.

Herein, we solve the above challenge by engineering an electricity-powered dual-mode slippery lubricant-impregnated porous surface (DM-SLIPS) composed of paraffin wax, superhydrophobic laser-ablated polytetrafluoroethylene (LA-PTFE) and an embedded silver nanowire thin-film heater. Taking advantage of its fast electric response, DM-SLIPS could be switched *in situ* to repel diverse liquids that dwelt on the surface under an ultralow voltage of 6 V. Simultaneously, the surface visibility could be fine-tuned between opaque and transparent selectively, termed respectively as "lock mode" and "release mode", in response to an electric trigger (Fig. 1). The underlying mechanism is that the paraffin tends to be melt within 20 s under the influence of Joule heating, forming a visible slippery air/liquid paraffin/solid substrate (ALS) system. Once the electric stimulus is discharged, paraffin solidification would result in a rough air/solid paraffin/solid platform (ASS) regime featuring higher reflectivity within 5 s. Thanks to its portability and high integrity, DM-SLIPS was able to remove surface-frozen ice within 4 min by *in situ* homogeneous Joule heating. Significantly, with the electricity-triggered DM-SLIPS cover, the temperature of the space inside the photo-thermal object could be reversibly switched between 34 °C and 29 °C by fine-tuning the solar energy input. In comparison with previously reported smart surfaces, the current electricity-powered ice-phobic water-repellent DM-SLIPS is more competent in harnessing *in situ* surface dynamic glazing and coping with thermal challenges under extreme climates.

2. Results and discussion

2.1. Facile fabrication of bioinspired DM-SLIPS for switching surface transparency and hysteresis

Inspired by the natural pitcher plant *Nepenthes*, the strategy developed for fabricating electricity-powered DM-SLIPS involved four crucial procedures, including programmable laser scanning, paraffin impregnation, silver-nanowire coating and adhesive bonding (Fig. 2A). Accordingly, the cost for fabri-

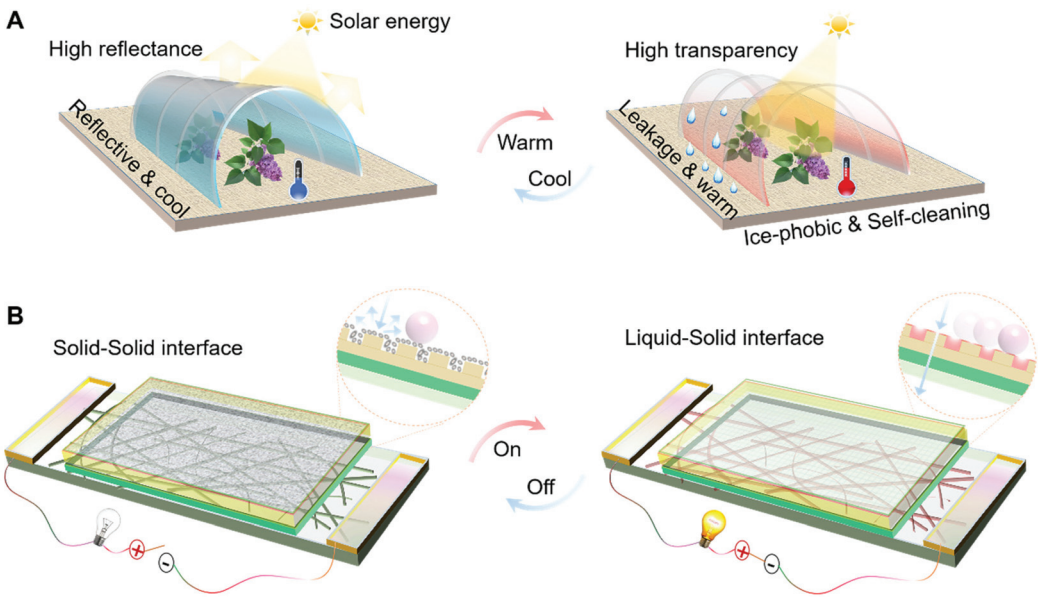

Fig. 1 Conceptual bioinspired intelligent greenhouse enabled by all-in-one DM-SLIPS. (A) Schematic diagram displaying that a multifunctional tent should block light on a dry sunny day but turn both transparent and water repellent on a dim rainy day, in addition to *in situ* de-icing on a snowy day. (B) Schematic diagram of the rational design of a water-proof, ice-phobic and transparency-switchable actuator. Inspired by natural *Nepenthes*, the dual-mode electric-powered tent is composed of paraffin wax, a superhydrophobic porous platform and an embedded flexible heater. Once its surface is impregnated, paraffin wax solidifies without Joule heating, while liquids/ice tend to stick on the surface and light is blocked. In sharp contrast, once the impregnated paraffin wax is liquefied upon Joule heating, liquids/ice roll off and light is allowed to pass. This strategy is convincingly adaptive for thermal management in extreme climates (*e.g.*, dim rainy days, snowy winter).

Published on 04 February 2022. Downloaded on 8/10/2024 8:31:31 AM.

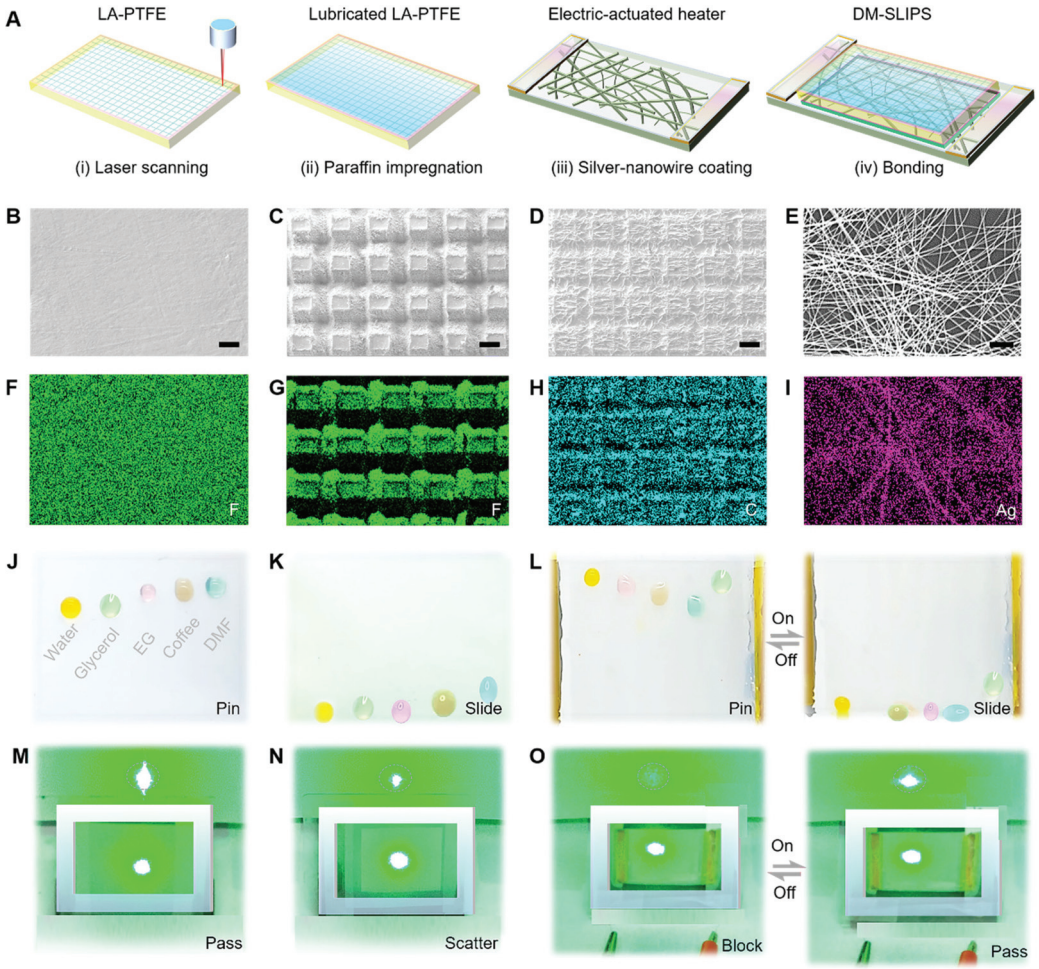

Fig. 2 Fabrication of DM-SLIPS by combining a fs laser-based manufacturing technique and a transparent silver-nanowire thin-film heater. (A) Schematic strategy for preparing electric-triggered DM-SLIPS, including laser scanning for superhydrophobic micropillar-arrayed LA-PTFE, paraffin impregnation for a temperature-responsive slippery surface, weaving an electric-actuated silver-nanowire thin-film heater and integrating the resultant slippery surface together with a transparent heater. SEM images of (B) pristine PTFE, (C) laser-ablated PTFE, (D) paraffin-impregnated LA-PTFE and (E) the as-prepared silver nanowires. The scale bars are respectively 50, 50, 50 and 1 μm. (F–I) The corresponding EDS maps of the elements F, F, C and Ag. The motion behavior of diverse liquids on inclined (J) pristine PTFE, (K) LA-PTFE and (L) discharged DM-SLIPS and powered DM-SLIPS (6 V). Digital pictures presenting the transmittance of a Green laser irradiated on the surfaces of (M) pristine PTFE, (N) LA-PTFE and (O) discharged DM-SLIPS and powered DM-SLIPS (6 V). The results reveal that electric-powered DM-SLIPS is more competent in reversibly switching surface adhesion and light properties synergistically.

cating a slice of DM-SLIPS (6 cm × 6 cm) was roughly estimated at ~$3.7 (Fig. S15†).

Concretely, a piece of smooth PTFE membrane was engineered to have a highly uniform micropillar-arrayed morphology by using the one-step femtosecond (fs) laser cross-scanning method, thereby obtaining a periodic nano/micro-structured LA-PTFE (Fig. 2B and C and Fig. S1†). Notably, robust SLIPS has to possess a superhydrophobic porous platform to prevent the intrusion of the surface-targeted liquids.[21] To obtain an optimized water-proof LA-PTFE substrate, the influence of laser scanning interval on surface wettability was systematically investigated (Fig. S2†). Thereby, the pillar length, width, height and interval of the optimized LA-PTFE substrate were characterized to be 49.5, 50, 51.2 and 100.8 μm, respectively. The elemental map of LA-PTFE further indicated that the fluorine element had an apparent periodic distribution compared with that in pristine smooth PTFE (Fig. 2F and G). After normalizing the atomic ratio of F relative to C, the decrease in C atoms in LA-PTFE signified that femtosecond laser ablation was conducive to modifying the wettability by erasing the surface-water-affinitive organics, in addition to introducing micro/nano-structures (Fig. S3†). In comparison with traditional chemical fluorination, the current fs laser manufacturing technology has been widely adopted for various materials since it is competent in generating robust superwetting micro/nano-structured topographies with durable longevity.[22–24] By the thermal-spinning method, paraffin wax (~2.3 g), which behaves as a temperature-responsive phase-changing material, could be homogeneously impregnated into the as-obtained LA-PTFE substrate based on the giant capillary

 This journal is © The Royal Society of Chemistry 2022

Published on 04 February 2022. Downloaded on 8/10/2024 8:31:31 AM.

force, and the thickness of impregnated paraffin was measured as ~33.5 μm (Fig. 2D and H and Fig. S4†). Thereafter, according to the classical polyol method described in our previous work,[25] high-quality ultra-thin silver nanowires (~21 nm) with a high aspect ratio (>1000) were harvested with ease (Fig. 2E and I). By employing a rheology-modified silver nanowire ink (1 mg mL^{-1}), we could further weave a highly transparent conductive silver-nanowire network with a transmittance of 87.8% at a wavelength of 550 nm and sheet resistance of 63.3 Ω sq^{-1} (Fig. S5†). On this basis, a silver-nanowire-based thin-film heater was fabricated by introducing two symmetric copper wires bridged with thermo-cured silver paste. Accordingly, the flexible electricity-powered DM-SLIPS could be successfully integrated by laminating the silver nanowire thin-film heater with the paraffin-lubricated LA-PTFE using a binding layer (Fig. S6†). Significantly, unlike the single functionalities of PTFE (higher adhesion) or LA-PTFE (lower hysteresis), DM-SLIPS was more competent in realizing dynamic motion control between pinning and sliding in terms of diverse liquids (Fig. 2J–L and Fig. S7; ESI, Movie S1†). Fig. 2M displays the remote circular laser irradiating pristine PTFE, which allowed the most penetration of incident light owing to minimum scattering due to relatively flat topography. Once treated with programmed laser scanning, LA-PTFE acquired a light-scattering terrain, and the penetrating light spot could be tailored to a contracted spot (Fig. 2N). Further, we hybridized the light-scattering paraffin wax into the as-prepared LA-PETF to construct a reflective air/solid paraffin/solid LA-PTFE (ASS) system for completely blocking the incident light, and this could be *in situ* switched to a 'release mode' with the help of Joule heating, resulting in a semitransparent air/liquefied paraffin/solid LA-PTFE (ALS) system (Fig. 2O; ESI, Movie S2†). Notably, compared with PTFE and LA-PTFE, DM-SLIPS serves as an intelligent actuator and has the advantage of a switchable optical property, which is a significant prerequisite for thermal management through allowing/blocking the outdoor incident light. Moreover, we have experimentally and theoretically investigated the durability of the as-prepared electric-powered DM-SLIPS (Fig. S13; ESI, Movie S6†). An intuitive method was designed to verify if loss of paraffin wax occurred with Joule-heat-induced melting in erectly installed DM-SLIPS with repeated loading/discharging of electrical stimulus. As seen in Fig. S13a,† 5 cycles of paraffin solidification/melting operation were implemented for ~20 min, and the transparency of DM-SLIPS always switched between the "lock mode" and "release mode". This result signified that no apparent loss of paraffin wax occurred during the cyclic melting process, thereby revealing the longevity of the current DM-SLIPS material. Meanwhile, the 3D laser profiles of DM-SLIPS subjected to cyclic solidification/melting operation verified the good durability of the current smart window (Fig. S13c†). In view of fluid dynamics, the giant capillary force (F_C) arising from the micro/nano-structures in LA-PTFE together with the viscous force (F_{Vis}) in melting paraffin wax may easily overcome gravity (F_g). They corporately contributed to the good stability of the switchable DM-SLIPS (Fig. S13b†).

2.2. Switching thermodynamics for diverse liquids on ice-phobic DM-SLIPS

Thermal infrared imaging displayed the surface radiant heat variation on DM-SLIPS in response to an alternating electricity trigger (6 V), thereby demonstrating the homogeneous generation and rapid removal of Joule heat (Fig. 3A). By recording the *in situ* temperature evolution as a function of charging duration, we detected that DM-SLIPS showed a fast thermal response to the external electrical input (Fig. 3B). That is, when we loaded the electric current *in situ*, the surface temperature could be elevated from room temperature to the melting point of paraffin wax (T_M) within 20 s. Once the power was discharged, the surface temperature tended to decay and form a temperature plateau below the T_M within 5 s. Thereby, DM-SLIPS could be switched between an undulant frictional state and a smooth slippery one by regulating the surface horizontal resistance force between a larger f_{SL} (f_{SL} denotes the frictional force between solidified paraffin and the manipulated liquids) and a smaller f_{LL} (f_{LL} refers to the frictional force between liquefied paraffin and the manipulated liquids) (Fig. 3C). In addition, by alternately applying/discharging electricity, we quantitatively studied the f_{LL} and f_{SL} curves for diverse liquids, including water, glycerol, ethylene glycol (EG) and dimethyl formamide (DMF), on the horizontal planar DM-SLIPS surface (Fig. 3D and E). Accordingly, their corresponding values of f_{SL} and f_{LL} were measured as 117.0, 109.7, 92.3, 51.9 μN and 23.0, 15.7, 14.6, 10.7 μN (Fig. S8†), respectively. The larger the surface tension, the greater was the resistance force. Based on the above-explored fundamental considerations, thermodynamics over de-icing was further investigated using DM-SLIPS mounted on a Peltier semiconductor chilling plate (Fig. 3F; ESI, Movie S3†). We experimentally evidenced that DM-SLIPS could be switched to an ice-phobic slippery surface within 1 min with the aid of Joule heating. Accordingly, we experimentally recorded the temperature variation in DM-SLIPS with Joule-heating time when installed in simulated cold weather (−20 °C) (Fig. S12; ESI, Movie S5†). The result indicated that the surface temperature increased exponentially with the Joule-heating duration. Notably, the recorded data evidenced that the time consumed by DM-SLIPS to heat up from −20° to 0° (a given theoretical ice melt point) was ~56 s, which is highly consistent with our experimental result.

2.3. Fine-tuning the optical property of electricity-triggered DM-SLIPS

Apart from the water-repellent and ice-phobic merits, DM-SLIPS could simultaneously and reversibly fine-tune the surface transmissivity in response to an electric trigger of 6 V (Fig. S9†). As shown in Fig. 4A, the laser-textured PTFE contributes to the decrease in optical visibility in comparison with that of pristine PTFE owing to the introduction of nano/micro-structures. Typically, the transmittance at 600 nm wavelength for pristine PTFE and LA-PTFE were 79.6% and 67.4%, respectively. After impregnating paraffin wax into the micro/nano-structured LA-PTFE, the discharged DM-SLIPS presented

Published on 04 February 2022. Downloaded on 8/10/2024 8:31:31 AM.

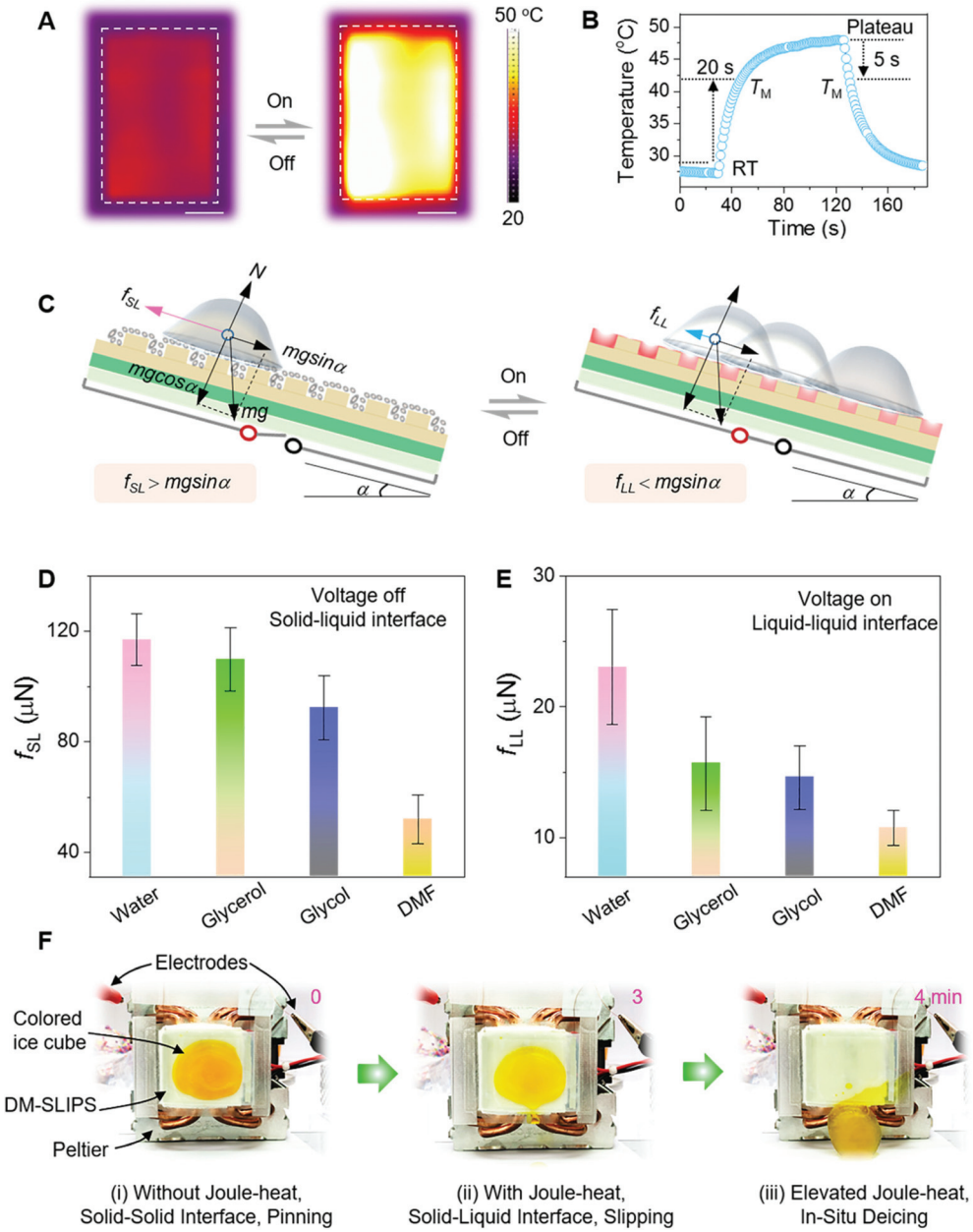

Fig. 3 Thermodynamics of switching the surface adhesion of liquids/ice. (A) IR images displaying the temperature variation in DM-SLIPS in response to electric stimulus (6 V); the scale bar is 1 cm. (B) Temperature evolution with charging/discharging duration to investigate the time consumed to melt/solidify the surface lubricant. (C) Force analysis in the cases of DM-SLIPS during the *in situ* loading and discharging of Joule heating. By the *in situ* application/removal of Joule heat, the resistance force could be switched between lower f_{LL} (liquid–liquid interface) and higher f_{SL} (solid–liquid interface) values with ease. Quantitative measurements of (D) f_{SL} and (E) f_{LL} in terms of liquid droplets (10 μL) on charging/discharging DM-SLIPS using water, glycerol, ethylene glycol and DMF. (F) A proof-of-concept for *in situ* de-icing by applying Joule heating on DM-SLIPS. This electric-responsive DM-SLIPS is competent in repelling surface liquid contaminants and removing surface-frozen ice *in situ*, which has rarely been demonstrated by previously reported materials.

decreased light transmittance at 60.6%, which is denoted as the "lock state". In sharp contrast, once electric stimulus was applied on DM-SLIPS, the transparency recovery was almost the same as that of pristine PTFE at 74.2%, namely the "release state". Moreover, the corresponding reflectance values at 600 nm wavelength for PTFE, LA-PTFE, off-mode and on-mode DM-SLIPS were recorded as 26.4%, 38.0%, 39.6% and 29.9% (Fig. 4B), respectively. Then, we investigated the influence of the pillar interval on the wettability and optical properties, for which the laser power and scanning speed were set at constant values of 150 mW and 2 mm s^{-1}, respectively, considering that the morphology of the micro-pillars, including their width (l), height (h) and interval (d), is determined by the programmable laser ablation process, which subsequently

 This journal is © The Royal Society of Chemistry 2022

Published on 04 February 2022. Downloaded on 8/10/2024 8:31:31 AM.

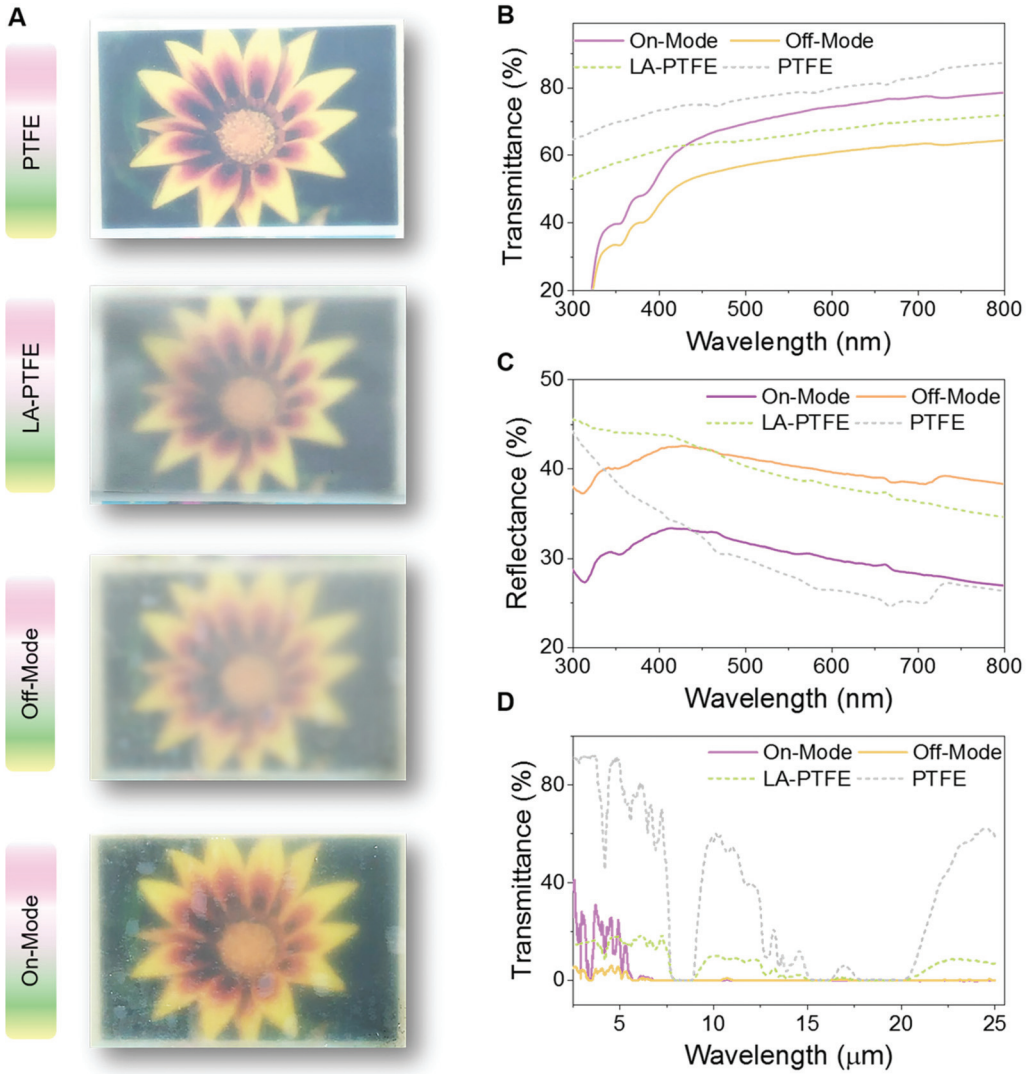

Fig. 4 Electricity-triggered transparency fine-tuning between the release mode and the lock mode. (A) Photographs displaying the visibility difference between pristine PTFE, LA-PTFE, charging DM-SLIPS and discharging DM-SLIPS. (B) Transmission spectra and (D) reflectance spectra in a wavelength range of 300–800 nm corresponding to these four surfaces. (C) Transmission spectra in a wavelength range of 2.5–25 μm. The results suggest that in comparison with pristine PTFE and LA-PTFE, DM-SLIPS not only has the minimum reflectance to visible light but also shows more intense resistance to IR light, signifying its better cooling performance as well as its great potential in IR camouflage.

affects the on–off transparency of DM-SLIPS by influencing the ratio of incident-light scattering and incident-light penetration (Fig. S16†). In theory, ① the stronger the laser power P, the larger would be the fs-laser-textured h, and thus the longer would be the light-scattering path in the grooves. As such, ② a slower scanning speed v would also contribute to elevated h and enhanced ablation scope, thereby deteriorating the transparency of DM-SLIPS. In short, the larger the laser power and scanning speed, the lower would be the transparency of DM-SLIPS but with a higher surface capillary force. Surface wettability and transparency are always paradoxical, indicating that the currently adopted parameters may not be an optimal selection. Apart from laser power and scanning speed, many other parameters also affect the optical and wetting properties of DM-SLIPS, such as the scanning cycle, laser pulse number, and laser dwelling time. Accordingly, we could further fine-tune the light-transmittance property by regulating the laser ablation parameters used for LA-PTFE in the subsequent study. Though the tuning amplitude was moderate, the emphasized advantage of DM-SLIPS could be attributed to its fast-responsive switching in terms of solar-light transmittance, analogous to a smart window. The switching range was not restricted to the visible spectrum (300–800 nm) but the material was also responsive in the short-wave near-infrared (SWNIR, 0.8–2.5 μm) and mid-infrared regions (MIR, 2.5–4.0 μm) (Fig. 4C and Fig. S10†). Notably, DM-SLIPS exhibited termination of the switch in the long-wave infrared range (LWIR, 8–13 μm), which could be ascribed to the strong reflec-

Published on 04 February 2022. Downloaded on 8/10/2024 8:31:31 AM.

tance of LWIR from the embedded silver nanowire network (Fig. 4D).[26] The exceptional thermal insulation endows DM-SLIPS with great potential for IR camouflage.[27–30] Significantly, the as-prepared DM-SLIPS is adaptive to planar and 3D terrains owing to its good flexibility, convincing that it would be a promising candidate for future flexible smart windows and other electronics (Fig. S14; ESI, Movie S7†).

2.4. Proof-of-concept for thermal management by activating DM-SLIPS on demand

To evaluate the feasibility of temperature regulation using DM-SLIPS, we showcase a proof-of-concept using a homemade system composed of a Fe_3O_4-doped PDMS membrane (3 wt%), 808 nm laser, electric power source and a computer-controlled

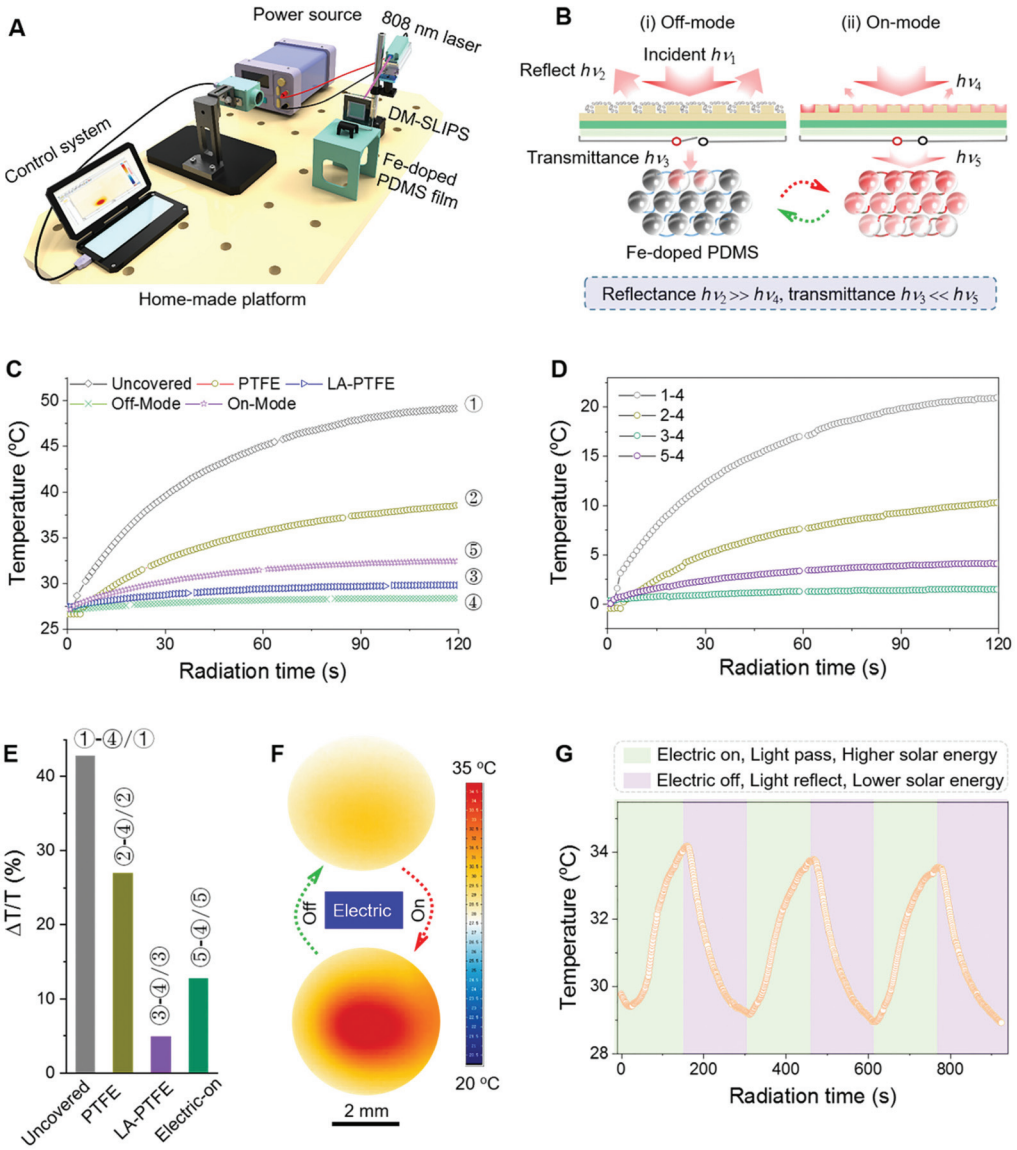

Fig. 5 Proof-of-concept for the DM-SLIPS shelter responsible for rational thermal management. (A) A homemade test system composed of a computer-controlled thermal IR imager, charging power source for triggering DM-SLIPS, 808 nm laser and Fe_3O_4-doped PDMS membrane. (B) The switching principle for realizing thermal management by selectively harvesting and reflecting solar irradiation depending on *in situ* charging/discharging of the DM-SLIPS shelter. With electricity on, a light release mode favorable for solar energy gain is achieved due to the intense photothermal effect. When the electricity is turned off, a light lock mode conducive to reflecting visible light back to the outer space is achieved. (C) Photothermal effect-induced temperature in terms of radiation time for air (uncovered), pristine PTFE, LA-PTFE, charging DM-SLIPS, and discharging DM-SLIPS shelters placed before the Fe_3O_4-doped PDMS membrane. (D) Temperature difference and (E) cooling amplitude of the Fe_3O_4-doped PDMS membrane sheltered by air (uncovered), pristine PTFE, LA-PTFE, and charged DM-SLIPS relative to that covered with discharged DM-SLIPS. (E) Thermal IR images and (F) temperature-time curve of the DM-SLIPS-sheltered Fe_3O_4-doped PDMS membrane in response to a cyclic electric trigger (6 V). The results show that the DM-SLIPS shelter exhibits a cooling temperature of 21.0 °C, superior to those of PTFE (10.6 °C) and LA-PTFE (19.4 °C). Significantly, this DM-SLIPS shelter is competent in reversibly switching the indoor temperature between 34 °C and 29 °C, thereby realizing selective solar energy gain/blockage.

This journal is © The Royal Society of Chemistry 2022

Published on 04 February 2022. Downloaded on 8/10/2024 8:31:31 AM.

thermal infrared imager (Fig. 5A and Fig. S11†). The underlying principle is that the DM-SLIPS shelter allows the transmittance of incident light in the "release mode", and the surface temperature of Fe_3O_4-doped PDMS exposed to intense 808 nm laser would increase by "solar radiative heating" in a manner relying on the photo-thermal effect (Fig. 5B). Once the DM-SLIPS shelter is switched to the "lock mode", its surface tends to reflect the incident light, producing a "solar-blocked shady cooling" effect. By respectively mounting the pristine PTFE, LA-PTFE and DM-SLIPS covers ahead of the Fe_3O_4-doped PDMS platform, we detected that the corresponding maximum temperatures were 49.1 °C (uncovered, air medium), 38.5 °C, 29.7 °C and 28.2 °C (Fig. 5C).

Compared to the pristine PTFE and LA-PTFE covers, which correspondingly reduced the temperature by 10.6 °C and 19.4 °C, the DM-SLIPS shelter showed a superior difference of 21.0 °C. Moreover, the temperature of the indoor photo-thermal platform covered with the DM-SLIPS shelter could be reversibly fine-tuned between 34 °C and 29 °C by *in situ* loading/discharging an ultra-low voltage of 6 V (ESI, Movie S4†). We experimentally demonstrated that the discharged DM-SLIPS shelter had a remarkable cooling performance, with values 20.9 °C, 10.3 °C and 1.5 °C lower than those of the air (uncovered), pristine PTFE and LA-PTFE shelters, respectively (Fig. 5D). Furthermore, the cooling amplitude of the discharged DM-SLIPS shelter was superior to those of the air, PTFE and LA-PTFE shelters by as much as 42.8%, 26.9% and 4.9%, respectively (Fig. 5E). Significantly, cyclic switching of the DM-SLIPS shelter enables us to fine-tune the solar energy input, thereby regulating the indoor temperature on demand for personal comfort (Fig. 5F and G).

3. Conclusions

In summary, a bioinspired electricity-powered DM-SLIPS was fabricated by integrating superhydrophobic laser-ablated PTFE, temperature-responsive paraffin wax and an electricity-actuated silver-nanowire thin-film heater. Leveraging its fast electric response, DM-SLIPS could repel diverse liquid species that dwelt on the surface under an ultralow voltage of 6 V. Simultaneously, the light irradiating on DM-SLIPS could be fine-tuned between a "lock mode" and "release mode" based on the solidification/liquefication of paraffin wax. The underlying principle is that electricity-induced Joule heating would melt the lubricating paraffin wax within 20 s for the rapid formation of a transparent slippery ALS system. Once the electric power is remotely cut-off, the liquid paraffin would reconfigure to the solid state within 5 s, generating a reflective rough ASS regime. Moreover, DM-SLIPS was even capable of removing surface-dwelling frozen ice within 4 min depending on electricity-induced homogeneous Joule heating. Significantly, compared with the rigid PTFE and LA-PTFE shelters, the electricity-triggered DM-SLIPS was more competent in reversibly switching the temperature of the indoor photo-thermal object between 34 °C and 29 °C, thereby realizing rational thermal management on demand. Most recently, SLIPS combined with a triboelectric nanogenerator (TENG), namely SLIPS-TENG, has displayed applicability in energy-harvesting scenarios.[32] Therefore, our extreme-climate-adaptive DM-SLIPS shelter, with the water-proofing, transparency-switchable and ice-phobic merits, is envisioned to have application potential in vegetable greenhouses, smart windows, outdoor tents, IR camouflage, and energy recovery.

4. Experimental section

4.1. Materials

The polytetrafluoroethylene (PTFE) membranes (thickness: 100 μm) were donated by Shanghai Shenchen Rubber & Plastic Hardware Co., Ltd. $AgNO_3$ (99.8%) was obtained from Shanghai Qiangshun Chemical Reagent Co., Ltd. Polyvinylpyrrolidone (PVP, MW of 55 000) and hydroxypropyl methylcellulose (HPMC) were purchased from Sigma-Aldrich. Ethylene glycol (EG), glycerol, DMF, NaCl, NaBr, and acetone were purchased from Sinopharm Chemical Reagent Co., Ltd. Sago® 9760 and Sago® 3223 were obtained from Sago Co., Ltd. The silver paste was brought from Shenzhen Sinwe New Material Co., Ltd. Paraffin wax ($T_m \sim 40$–$42°$) was provided by Jinan Dingyi Chemical Co., Ltd. The Fe_3O_4 nanoparticles (diameter: 10 nm) were contributed by Tianjin Kaili Metallurgical Research Institute. Double-faced adhesive tape (thickness: 100 μm) obtained from Yunan tape Co., Ltd was used as the bonding agent. Distilled water (H_2O, 1 g cm^{-3} density) was used for contact-angle tests on the materials.

4.2. Femtosecond laser engineering of superhydrophobic LA-PTFE

The micropillar-arrayed LA-PTFE was manufactured by the cross-scanning method using a femtosecond laser. The laser beam (104 fs, 1 kHz, 800 nm) from a regenerative amplified Ti: sapphire femtosecond laser system (Legend Elite-1K-HE, Coherent) was employed for ablation. During the fabrication process, the laser beam was guided onto the PTFE surface *via* a galvanometric scanning system (SCANLAB), which made the laser beam focus and scan along the *x*/*y* coordinate direction. The scanning interval, that is, the spacing between two adjacent lines ranged from 0.1 to 0.3 mm. The laser power and scanning rate were respectively fixed at 150 mW and 2 mm s^{-1}.

4.3. Building of Electricity-powered DM-SLIPS

Synthesis of ultra-thin silver nanowires. For synthesis, (A) 0.220 M NaBr, (B) 0.210 M NaCl, and (C) 0.505 M PVP in EG were individually prepared for utilization. Fresh $AgNO_3$ was dissolved in EG in an ice-cold ultrasonic bath (4–8 °C) for 5 min. Subsequently, 2.5 mL of A, 5 mL of B, 25 mL of C, and 25 mL of $AgNO_3$ (0.265 M) were successively added to a 100 mL flask placed in an oil bath at room temperature. Vigorous stirring was applied for 30 min, and then, the temperature in the flask was elevated to 170 °C in 15 min, while nitrogen gas at a flux of 150 mL min^{-1} was bubbled through

Published on 04 February 2022. Downloaded on 8/10/2024 8:31:31 AM.

the reaction mixture. Thereafter, the flask was corked, and the reaction was left to proceed for 1 h without disturbance. The flask was taken off the oil bath immediately and transferred to the water for cooling once the reaction was terminated.[25]

Formulation of silver nanowire ink. A total of 16 mg of purified silver nanowires harvested by positive-pressure filtration and an acetone purification procedure were dissolved in 16 mL of DI water with the assistance of 32 mg of hydroxypropyl methylcellulose (HPMC), a Sago-dispersant (v/v 0.0025%), and a Sago-flatting agent (v/v 0.0025%). Finally, 1 mg mL^{-1} silver nanowire ink could be obtained after the mixture was fixed on a table concentrator and allowed to blend for 1.5 h at a rotating speed of 110 rpm.[25]

Preparation of the transparent silver-nanowire thin-film heater. An automatic coating machine (BEVS 1811/2) equipped with an OSP-30 scraper was utilized to coat the conductive silver nanowire network on a flexible polyethylene terephthalate (PET) substrate, and the coating rate and area were fixed at 50 mm s^{-1} and A4 (21.0 cm × 29.7 cm), respectively.[25] The start button was pressed after dropping 1 mL of the silver nanowire ink, and a highly conductive silver-nanowire film was obtained after a brief annealing process at 60 °C for 5 min; the film was tailored to an area of ~4 cm × 6 cm for use. Thereafter, two symmetric copper-wire electrodes were soldered using the patterned oblong silver paste. The silver-nanowire heater could be prepared after annealing at 70 °C for 5 h, and was then integrated with the as-prepared LA-PTFE by binding them with double-sided tape (thickness: 100 μm).

Thermal-spin-coating of paraffin wax. LA-PTFE embedded with the silver-nanowire heater was fixed on a glass slide by the 3 M adhesive tape. Then, a patch of solid paraffin wax (~2.3 g) was placed on this surface and allowed to melt and spread for 5 min under an infrared (IR) lamp; the distance between the IR lamp and sample was fixed at ~8 cm. Thereafter, the spin-coating program (time: 5 min; speed: 1200 rpm) was initiated. Finally, DM-SLIPS composed of paraffin-impregnated LA-PTFE as the top layer, the adhesive binder as the middle layer and an underlying heater could be obtained after a condensation process at room temperature.

4.4. Characterization

The morphology of the silver nanowires, PTFE and micro/nanostructured LA-PTFE was characterized by using a field-emission scanning electron microscope (JSM-6700F). The mapping of the elements was conducted by energy-dispersive spectroscopy (SU8010/Aztec(X-MaxN)). The sliding angles of water on DM-SLIPS were measured using a CA100C contact-angle system (Innuo) at 10% humidity and 20 °C. The sheet resistance of the silver-nanowire film was measured using the four-point probe technique (RST-9, Four-Probe Technology). Surface temperature monitoring was achieved by a thermal infrared camera (VarioCAMhr head 680, InfraTec). The optical transmittance and reflectance curves were recorded by a UV-Visible spectrophotometer (UV-2501PC/2550, Shimadzu Corporation, Japan). Freezing the surface water droplets on DM-SLIPS to ice cubes was enabled by a Peltier board module (XD-36, Xingda Hengye Technology Co., Ltd, China). A near-infrared light (FU808AD300-BC/BD10, Fuzhe Technology Co., Ltd, China) with a wavelength of 808 nm (0.3 W; spot area, 1.4 × 2.3 mm^2) was used for the proof-of-concept experiment of DM-SLIPS serving as the light shutter. All digital photos were shot by a mobile phone (iPhone-8 plus, 7 mega-pixel). The 3D images used for monitoring the profile evolution of PTFE and LA-PTFE were captured by a 3D profile meter (VK-X100, KEYENCE CORPORATION, Japan).

Author contributions

C. C. and Y. Z. conceived of and designed the experiments. C. C., Y. C., H. Y., Q. S. and C. J. performed the experiments. C. C. and Y. Z. wrote the manuscript.

Conflicts of interest

There are no conflicts to declare.

Acknowledgements

This work was supported by the National Natural Science Foundation of China (No. 52005475), National Key Scientific Instrument and Equipment Development Project (No. 61927814). We acknowledge the Experimental Center of Engineering and Material Sciences at USTC for the fabrication and measuring of samples.

References

1 T. Ramesh, R. Prakash and K. K. Shukla, Life cycle energy analysis of buildings: An overview, *Energy Build.*, 2010, **42**, 1592–1600.
2 R. Baetens, B. P. Jelle and A. Gustavsen, Properties, requirements and possibilities of smart windows for dynamic daylight and solar energy control in buildings: A state-of-the-art review, *Sol. Energy Mater. Sol. Cells*, 2010, **94**, 87–105.
3 K.-S. Ahn, S. J. Yoo, M.-S. Kang, J.-W. Lee and Y.-E. Sung, Tandem dye-sensitized solar cell-powered electrochromic devices for the photovoltaic-powered smart window, *J. Power Sources*, 2007, **168**, 533–536.
4 A. Piccolo, Thermal performance of an electrochromic smart window tested in an environmental test cell, *Energy Build.*, 2010, **42**, 1409–1417.
5 J. Wang, L. Zhang, L. Yu, Z. Jiao, H. Xie, X. W. Lou and X. W. Sun, A bi-functional device for self-powered electrochromic window and self-rechargeable transparent battery applications, *Nat. Commun.*, 2014, **5**, 4921.
6 C. M. Lampert, Large-area smart glass and integrated photovoltaics, *Sol. Energy Mater. Sol. Cells*, 2003, **76**, 489–499.

 This journal is © The Royal Society of Chemistry 2022

Published on 04 February 2022. Downloaded on 8/10/2024 8:31:31 AM.

7 M.-H. Yeh, L. Lin, P.-K. Yang and Z. L. Wang, Motion-driven electrochromic reactions for self-powered smart window system, *ACS Nano*, 2015, **9**, 4757–4765.
8 S. Chen, Z. Wang, H. Ren, Y. Chen, W. Yan, C. Wang, B. Li, J. Jiang and C. Zou, Gate-controlled VO_2 phase transition for high-performance smart windows, *Sci. Adv.*, 2019, **5**, eaav6815.
9 F. Guo, S. Chen, Z. Chen, H. Luo, Y. Gao, T. Przybilla, E. Spiecker, A. Osvet, K. Forberich and C. J. Brabec, Printed smart photovoltaic window integrated with an energy-saving thermochromic layer, *Adv. Opt. Mater.*, 2015, **3**, 1524–1529.
10 Y. Gao, H. Luo, Z. Zhang, L. Kang, Z. Chen, J. Du, M. Kanehira and C. Cao, Nanoceramic VO_2 thermochromic smart glass: A review on progress in solution processing, *Nano Energy*, 2012, **1**, 221–246.
11 H. Kim, Y. Kim, K. S. Kim, H. Y. Jeong, A.-R. Jang, S. H. Han, D. H. Yoon, K. S. Suh, H. S. Shin and T. Kim, Flexible thermochromic window based on hybridized VO_2/graphene, *ACS Nano*, 2013, **7**, 5769–5776.
12 J. Zhu, Y. Zhou, B. Wang, J. Zheng, S. Ji, H. Yao, H. Luo and P. Jin, Vanadium dioxide nanoparticle-based thermochromic smart coating: High luminous transmittance, excellent solar regulation efficiency, and near room temperature pase transition, *ACS Appl. Mater. Interfaces*, 2015, **7**, 27796–27803.
13 H. Khandelwal, R. C. Loonen, J. L. Hensen, M. G. Debije and A. P. Schenning, Electrically switchable polymer stabilised broadband infrared reflectors and their potential as smart windows for energy saving in buildings, *Sci. Rep.*, 2015, **5**, 11773.
14 Y. Kim, D. Jung, S. Jeong, K. Kim, W. Choi and Y. Seo, Optical properties and optimized conditions for polymer dispersed liquid crystal containing UV curable polymer and nematic liquid crystal, *Curr. Appl. Phys.*, 2015, **15**, 292–297.
15 S. Park and J. W. Hong, Polymer dispersed liquid crystal film for variable-transparency glazing, *Thin Solid Films*, 2009, **517**, 3183–3186.
16 D. J. Gardiner, S. M. Morris and H. J. Coles, High-efficiency multistable switchable glazing using smectic A liquid crystals, *Sol. Energy Mater. Sol. Cells*, 2009, **93**, 301–306.
17 H.-K. Kwon, K.-T. Lee, K. Hur, S. H. Moon, M. M. Quasim, T. D. Wilkinson, J.-Y. Han, H. Ko, I.-K. Han, B. Park, B. K. Min, B.-K. Ju, S. M. Morris, R. H. Friend and D.-H. Ko, Optically switchable smart windows with integrated photovoltaic devices, *Adv. Energy Mater.*, 2015, **5**, 1401347.
18 X. Yao, Y. Hu, A. Grinthal, T. S. Wong, L. Mahadevan and J. Aizenberg, Adaptive fluid-infused porous films with tunable transparency and wettability, *Nat. Mater.*, 2013, **12**, 529–534.
19 X. Yao, J. Ju, S. Yang, J. Wang and L. Jiang, Temperature-driven switching of water adhesion on organogel surface, *Adv. Mater.*, 2014, **26**, 1895–1900.
20 K. Manabe, T. Matsubayashi, M. Tenjimbayashi, T. Moriya, Y. Tsuge, K. H. Kyung and S. Shiratori, Controllable broadband optical transparency and wettability switching of temperature-activated solid/liquid-infused nanofibrous membranes, *ACS Nano*, 2016, **10**, 9387–9396.
21 T. S. Wong, S. H. Kang, S. K. Tang, E. J. Smythe, B. D. Hatton, A. Grinthal and J. Aizenberg, Bioinspired self-repairing slippery surfaces with pressure-stable omniphobicity, *Nature*, 2011, **477**, 443–447.
22 C. Chen, Z. Huang, L. A. Shi, Y. Jiao, S. Zhu, J. Li, Y. Hu, J. Chu, D. Wu and L. Jiang, Remote photothermal actuation of underwater bubble toward arbitrary direction on planar slippery Fe_3O_4-doped surfaces, *Adv. Funct. Mater.*, 2019, **29**, 1904766.
23 J. Yong, C. Zhang, X. Bai, J. Zhang, Q. Yang, X. Hou and F. Chen, Designing "supermetalphobic" surfaces that greatly repel liquid metal by femtosecond laser processing: Does the surface chemistry or microstructure play a crucial role?, *Adv. Mater. Interfaces*, 2020, **7**, 1901931.
24 J. Wu, J. He, K. Yin, Z. Zhu, S. Xiao, Z. Wu and J. A. Duan, Robust hierarchical porous PTFE film fabricated via femtosecond laser for self-cleaning passive cooling, *Nano Lett.*, 2021, **21**, 4209–4216.
25 C. Chen, Y. Zhao, W. Wei, J. Tao, G. Lei, D. Jia, M. Wan, S. Li, S. Ji and C. Ye, Fabrication of silver nanowire transparent conductive films with an ultra-low haze and ultra-high uniformity and their application in transparent electronics, *J. Mater. Chem. C*, 2017, **5**, 2240–2246.
26 A. Yang, L. Cai, R. Zhang, J. Wang, P. C. Hsu, H. Wang, G. Zhou, J. Xu and Y. Cui, Thermal management in nanofiber-based face mask, *Nano Lett.*, 2017, **17**, 3506–3510.
27 L. Xiao, H. Ma, J. Liu, W. Zhao, Y. Jia, Q. Zhao, K. Liu, Y. Wu, Y. Wei, S. Fan and K. Jiang, Fast adaptive thermal camouflage based on flexible VO(2)/Graphene/CNT Thin Films, *Nano Lett.*, 2015, **15**, 8365–8370.
28 O. Salihoglu, H. B. Uzlu, O. Yakar, S. Aas, O. Balci, N. Kakenov, S. Balci, S. Olcum, S. Suzer and C. Kocabas, Graphene-based adaptive thermal camouflage, *Nano Lett.*, 2018, **18**, 4541–4548.
29 Y. Qu, Q. Li, L. Cai, M. Pan, P. Ghosh, K. Du and M. Qiu, Thermal camouflage based on the phase-changing material GST, *Light: Sci. Appl.*, 2018, **7**, 26.
30 K. K. Du, Q. Li, Y. B. Lyu, J. C. Ding, Y. Lu, Z. Y. Cheng and M. Qiu, Control over emissivity of zero-static-power thermal emitters based on phase-changing material GST, *Light: Sci. Appl.*, 2017, **6**, e16194.
31 Y. Wang, L. Zhang, Y. Guo, Y. Gan, G. Liu, D. Zhang and H. Chen, Air bubble bridge-based bioinspired underwater adhesion, *Small*, 2021, **17**, 2103423.
32 W. Xu, X. Zhou, C. Hao, H. Zheng, Y. Liu, X. Yan, Z. Yang, M. Leung, X. C. Zeng, R. X. Xu and Z. Wang, SLIPS-TENG: robust triboelectric nanogenerator with optical and charge transparency using a slippery interface, *Natl. Sci. Rev.*, 2019, **6**, 540–550.